RSC Advances

PAPER

View Article Online
View Journal | View Issue

Cite this: *RSC Adv.*, 2023, **13**, 2311

A novel and sensitive ratiometric fluorescent quantum dot-based biosensor for alkaline phosphatase detection in biological samples *via* the inner-filter effect†

Penghui Hu,[ab] Ruiyan Huang,[ab] Ye Xu,[ab] Tengfei Li,[c] Jun Yin,[ab] Yu Yang,[ab] Yuan Liang,[ab] Xiaohan Mao,[d] Li Ding [ab] and Chang Shu *[ab]

Alkaline phosphatase (ALP) is an important biomarker whose abnormal level in activity is associated with hepatobiliary, skeletal, and renal diseases as well as cancer. Herein, we synthesized ZnSe@ZnS quantum dots (ZnSe@ZnS QDs) and Mn-doped ZnS quantum dots (Mn:ZnS QDs) as fluorophores to establish the ratiometric fluorescent assay for ALP activity detection in biological samples. *p*-Nitrophenyl phosphate (PNPP) was used as a substrate for ALP, and the overlaps between absorption spectra of PNPP and excitation spectra of QDs resulted in sharp fluorescence quenching. Under the catalysis of ALP, PNPP was hydrolyzed into *p*-nitrophenol (PNP), which caused a red shift of absorption band of PNPP and fluorescence recovery of Mn:ZnS QDs (585 nm). However, the overlaps between absorption spectra of PNP and emission spectra of ZnSe@ZnS QDs led a further quenching of ZnSe@ZnS QDs (405 nm). Therefore, the ratiometric fluorescent signals (F_{585}/F_{405}) were associated with activity of ALP based on bidirectional responses of QDs to the concentration of PNPP. Under the optimum conditions, the method exhibited a good linear relationship from 4 to 96 U per L ($R^2 = 0.9969$) with the detection limit of 0.57 U per L. Moreover, the method was successfully applied for detecting the ALP activity in a complex biological matrix (human serum and HepG2 cells) with impressive specificity. In particular, the complicated chemical modifications of QDs and pretreatments of biological samples were not required in the whole detection procedures. Therefore, it not only provided a sensitive, specific and simple approach to clinical ALP activity detection, but it also provided support for early diagnosis of diseases.

Received 2nd November 2022
Accepted 3rd January 2023

DOI: 10.1039/d2ra06956c

rsc.li/rsc-advances

Introduction

Alkaline phosphatase (ALP) is an important biomarker,[1] and abnormal level of ALP activity is associated with hepatobiliary, skeletal diseases, kidney diseases and cancer. Therefore, convenient, sensitive and highly selective ALP activity detection is critical for clinical diagnosis. Colorimetry, electrochemistry and fluorometry methods have been used to detect ALP activity.[2,3] However, low sensitivity of colorimetry and complex chemical modifications of electrochemistry limited their applications. Fluorometry has been widely used in detection of biological macromolecules with high sensitivity and simple operations. Conventional fluorescent assays are usually limited by the poor photostability,[4] and the influence of biological substrates on fluorophores is also nonnegligible. In recent years, quantum dots (QDs) have attracted attention owning to excellent photostability, water dispersibility and bright fluorescence,[5,6] and have been used in the detection of drugs,[7,8] biomarkers,[9] viruses[10] *etc.* In most fluorometry related to QDs, the enhancement or attenuation of fluorescent signal depends on the interaction between QDs and analytes or intermediate molecules. An effective way to achieve specific interactions is to couple QDs with molecular imprinted polymers,[11] aptamers,[12] antibodies[13] or other recognition tools. Unfortunately, the coupling processes tend to result in aggregation or quenching of QDs. In fact, building high-quality recognition tools functionalized QDs is still a challenge.[14] In addition, the fluorescent signals are easily affected by environmental factors and

[a]*Key Laboratory of Drug Quality Control and Pharmacovigilance (China Pharmaceutical University), Ministry of Education, Nanjing 210009, China. E-mail: shuchang@cpu.edu.cn*

[b]*Department of Pharmaceutical Analysis, School of Pharmacy, China Pharmaceutical University, 24 Tongjiaxiang, Nanjing, 211198, P. R. China*

[c]*Department of Clinical Pharmacology, School of Pharmacy, Sir Run Run Hospital, Nanjing Medical University, Nanjing 211166, China*

[d]*Department of Pharmaceutical Engineering, School of Engineering, China Pharmaceutical University, Nanjing 211198, China*

† Electronic supplementary information (ESI) available: The FTIR spectra and cytotoxicity of QDs, optimization of condition for ALP activity detection, fluorescence quantum yield of QDs, comparison of performance of different analytical methods for ALP activity detection. See DOI: https://doi.org/10.1039/d2ra06956c

systematic errors, which lead to highly fluctuation of traditional fluorescent assay.[15]

Inner filtering effect (IFE) is due to the absorption of excitation or emission from fluorophores in the detection system. IFE can be caused by the overlapping between absorption spectra of the absorbers and fluorescence excitation or emission spectra of fluorophores.[16] IFE simplified the procedures of fluorescent assay and become a useful way to implement tag-free detection.[17] In addition, the wide excitation spectra and narrow emission spectra of QDs make it more flexible to establish a sensing system of fluorescent assay based on IFE.[18] In recent years, fluorometry based on IFE and QDs has been applied in the detection of pesticides,[19] therapeutic drugs[20] and biomarkers.[21] According to recent reports, the fluorescent assay has been used in the detection of ALP activity.[22,23] However, the nonnegligible interference from biological matrix on single-wavelength fluorescent signals still limited its application in complex biological samples. Actually, fluorescent assay based on IFE has been used in decreasing the interference from biological matrix and improving the specificity of ALP activity detection.[24] The ratiometric fluorescent assay considers the ratio of fluorescence intensity at multiple wavelengths as fluorescent signals, instead of the absolute values of fluorescence intensity at a single wavelength. Although the fluorescence intensity at a single wavelength usually increases or decreases in the present of interfering substances, the ratiometric fluorescent signals will not change obviously.[25] So far, ratiometric fluorescent assay has been used in detection of proteins and small molecules in biological matrix. Qian *et al.* reported a ratiometric fluorescent probe which recognized pantetheinase (Vanin-1) *via* the cleavage of peptide bonds and achieved *in situ* imaging of Vanin-1 with low interference and high specificity.[26] Yue *et al.* developed a dual-ratiometric fluorescent probe in which phenothiazine and azide were used as recognization tools for HClO and H_2S, which provided a specific approach to detect HClO and H_2S in cells.[27] Unfortunately, because of the wide emission spectra of organic fluorescent dyes, the overlaps of different fluorescence emission peaks usually caused significant interference between fluorescence channels, which seriously limited the sensitivity and accuracy of quantitative methods. Due to the large Stokes shift and narrow emission peaks of QDs, different fluorescence channels can be distinguished completely in ratiometric fluorescent assay. Consequently, developing a ratiometric fluorescent assay based on IFE and QDs is a prospective approach to achieve sensitive, simple, specific detection of ALP activity in biological matrix.

In this work, a ratiometric fluorescent assay based on IFE *via* ZnSe@ZnS QDs and Mn:ZnS QDs has been developed to detect ALP in biological samples. Firstly, the exciting light was absorbed by *p*-nitrophenyl phosphate (PNPP) competitively because of the overlaps between absorption spectra of PNPP and excitation spectra of QDs. Therefore, under the excitation of 310 nm illumination, QDs were quenched strongly. In the presence of ALP, PNPP was converted to *p*-nitrophenol (PNP), which caused a red shift of the absorption band from 310 nm to 405 nm. Then, the fluorescent emission of Mn:ZnS QDs (585 nm) recovered due to the consumption of PNPP. However, the overlap between the absorption spectra of PNP and the emission spectra of ZnSe@ZnS QDs resulted in a further decrease in the fluorescence intensity at 405 nm *via* IFE. Therefore, the ratio of fluorescence intensity (F_{585}/F_{405}) increased with the increase of ALP activity. The ratio of dual-wavelength fluorescence intensity (F_{585}/F_{405}) was considered as ALP activity related signals and a linear relationship was obtained with the detection limit of 0.57 U per L. In addition, the method exhibited good applicability in human serum samples and HepG2 lysate. Moreover, the performance in real samples of the method was compared with commercial kits and similar results was obtained, which indicated the great potential of our method in the detection of clinical samples. Owing to the impressive specificity and sensitivity of ratiometric fluorescent signals, the method provided a novel approach to the detection of ALP activity in complex biological matrix with low consumption and no pretreatment of samples.

Results and discussion

Characterization of ZnSe@ZnS QDs and Mn:ZnS QDs

JEM-2100F field emission transmission electron microscope (TEM, JEOL, Japan) was used for the characterization of morphology and size of QDs. The TEM images show the oil-dispersible and water-dispersible Mn:ZnS QDs are uniform spheric particles with the size of 3.68 ± 0.78 nm (Fig. 1A) and 4.49 ± 0.73 nm (Fig. 1B). Fig. 1C shows the microtopography of ZnSe@ZnS QDs, which are lightly agglomerated spheric particles with the size of 2.93 ± 0.50 nm. The EDS spectra of Mn:ZnS QDs obviously displays the characteristic spectral lines of manganese (Fig. S1A†), which indicates manganese has been doped into the nanocrystals. Fig. S1B† shows characteristic spectral lines of zinc, selenium and sulfur in ZnSe@ZnS QDs, which indicates the formation of ZnS shell.

The UV-visible absorption spectra, fluorescence spectra and fluorescence intensity were measured by SpectraMax M2e multimode reader (Molecular Devices, America). The optical

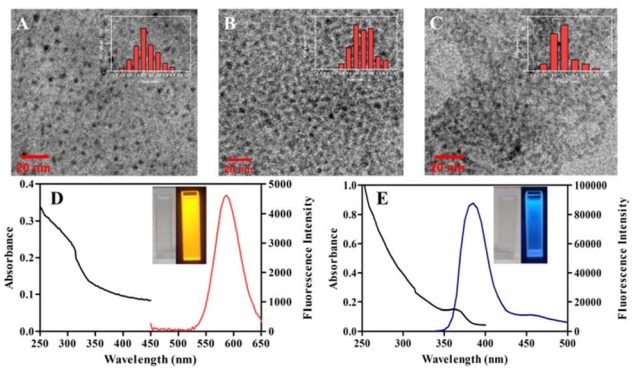

Fig. 1 The characterizations of Mn:ZnS QDs and ZnSe@ZnS QDs. The TEM images of oil-dispersible Mn:ZnS QDs (A), water-dispersible Mn:ZnS QDs (B) and ZnSe@ZnS QDs (C), respectively. The absorption and fluorescence emission spectra of water-dispersible Mn:ZnS QDs (D) and ZnSe@ZnS QDs (E), respectively. The insets in (D) and (E) are photographs of QDs solution under sunlight and UV-light at 254 nm.

properties of QDs are showed in Fig. 1, the maximum emission peaks of Mn:ZnS QDs and ZnSe@ZnS QDs are 585 nm and 385 nm, respectively. In addition, Fig. 1D shows the band edge absorption is located at 312 nm. According to the empirical equation reported by Suyver *et al.*, the size of Mn:ZnS QDs is estimated to be 3.60 nm, which is closed to the statistical size of oil-dispersible Mn:ZnS QDs (3.68 ± 0.78 nm) based on HRTEM.[28] However, the diameter of water-dispersible Mn:ZnS QDs increased significantly, which could be related to the slight aggregation of Mn:ZnS QDs in the ligand exchange and phase transition. Fig. 1E shows an absorption peak at 360 nm in the absorption spectra of ZnSe@ZnS QDs, which could be resulted from lowest-energy electron transition (1S peak) of ZnSe core.[29] Tables S1 and S2† show that the relative fluorescence quantum yields of Mn:ZnS QDs and ZnSe@ZnS QDs are 27.8% and 24.6%, which contribute to bright fluorescence stronger detection signals.

The FTIR spectra of QDs were characterized with IRTracer-100 Fourier transform infrared spectrometer (Shimadzu, Japan). The FTIR spectrum of oil-dispersible Mn:ZnS QDs shows the apparent peaks at 2850 cm^{-1}, 2918 cm^{-1}, 721 cm^{-1} (Fig. S2†), which are attributed to symmetric, asymmetric stretching vibration and bending vibration of methylene respectively. The bending vibration of methylene suggests the existence of long carbon chains of OAm on the surface of oil-dispersible Mn:ZnS QDs. However, the above apparent peaks disappear in water-dispersible Mn:ZnS QDs. In addition, the peak at 1732 cm^{-1} indicates the existence of carbonyl although the peak is not obviously. The above results show that OAm has been replaced by MPA successfully. The FTIR spectrum of ZnSe@ZnS QDs is shown in Fig. S2,† the peaks at 1604 cm^{-1} and 1398 cm^{-1} are attributed to asymmetric and symmetric stretching vibration of C=O in ionized carboxyl. The peaks at 1531 cm^{-1} and 1307 cm^{-1} are attributed to bending vibration of N–H and symmetric stretching vibration of C–N in amido bond. These results suggest that MPA and GSH coexist on the surface of QDs due to the imperfections of ZnS shell, which is consistent with previous reports.[30]

Feasibility for ALP detection

The feasibility for ALP detection based on IFE was assessed. The ZnSe@ZnS QDs and Mn:ZnS QDs were sharply quenched by 600 μM PNPP (Fig. 2A) because of the extensive overlap between absorption spectra of PNPP and excitation spectra of QDs (Fig. 2B). Line *c* in Fig. 2A showed that the fluorescence of Mn:ZnS QDs recovered in the presence of ALP. In the presence of ALP, PNPP was hydrolyzed into PNP, which caused red shift in absorption spectra of reaction system (Fig. 2C). Therefore, the IFE of PNPP on Mn:ZnS QDs gradually relieved with the hydrolyzation of PNPP. Line *b* and line *c* in Fig. 2D showed the overlap between absorption spectra of PNP and emission spectra of ZnSe@ZnS QDs, which caused IFE of PNP on ZnSe@ZnS QDs and the decreasing of fluorescence intensity once again. Briefly, the increasing of ratiometric fluorescent signals (F_{585}/F_{405}) caused by the contrary tendency of fluorescence intensity between Mn:ZnS QDs and ZnSe@ZnS QDs with

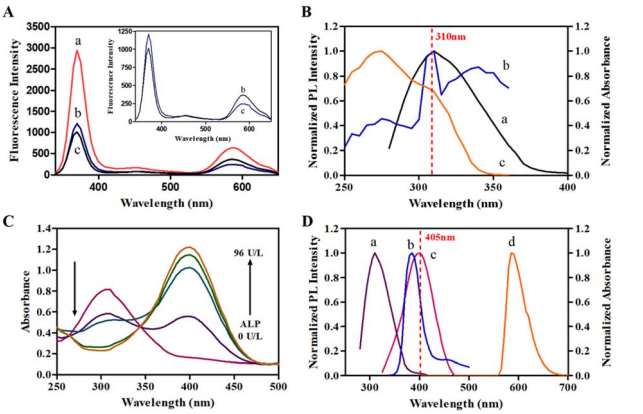

Fig. 2 The feasibility for ALP detection based on inner filter effect. (A) The fluorescence spectra of ZnSe@ZnS QDs and Mn:ZnS QDs in the presence of different substances. (a) None, (b) PNPP (600 μM), (c) PNPP (600 μM) and ALP (100 U per L). (B) The absorption spectrum of PNPP (a) and the excitation spectra of ZnSe@ZnS QDs (b), Mn:ZnS QDs (c). (C) The absorption spectra of incubation mixture in the presence of various activites of ALP (from bottom to top, 0, 16, 32, 64, 96 U per L). (D) The absorption spectra of PNPP (a), PNP (c) and the emission spectra of ZnSe@ZnS QDs (b), Mn:ZnS QDs (d).

the hydrolyzation of PNPP catalyzed by ALP. Therefore, the fluorescent signals were correlated with ALP activity.

Ratiometric fluorescent assay of ALP activity

In order to achieve a lower limit of detection and higher sensitivity, the pH, temperature, concentration of PNPP and reaction time were optimized. The activity of ALP was seriously affected by pH and temperature, hence the pH and temperature were optimized at first. The ratiometric fluorescence signals (R/R_0) reached the maximum value when the pH was 10.0 (Fig. S3A†) and the temperature was 37 °C (Fig. S3B†). According to the report, alkaline solution provided enough hydroxyl ions for dephosphorylation of substrates and contributed to enhance the activity of ALP.[31] Therefore, stronger ratiometric fluorescence signals were obtained due to the enhancement of ALP activity under the optimum pH and temperature.

The effects of concentration of PNPP in incubation buffer on ratiometric fluorescence signals were complex. On the one hand, weaker signals were obtained because of the slower reaction rate of dephosphorylation when the concentration of substrate (PNPP) was too low. On the other hand, when the concentration of PNPP was too high, the changes of ratiometric fluorescence signals were unconspicuous because of the low consumption rate of PNPP, which could still quench the fluorescence of ZnSe@ZnS QDs and Mn:ZnS QDs completely even after incubation. As shown in Fig. S3C,† the values of R/R_0 gradually increased with the increasing of concentration of PNPP until it was up to 600 μM, hence 600 μM PNPP was selected for following detection. Finally, the incubation time was optimized to reduce analysis period. Fig. S3D† clearly showed that the values of R/R_0 increased with the extension of incubation time. When the incubation time was longer than 75 min, the values of R/R_0 hardly increased. Therefore, 75 min

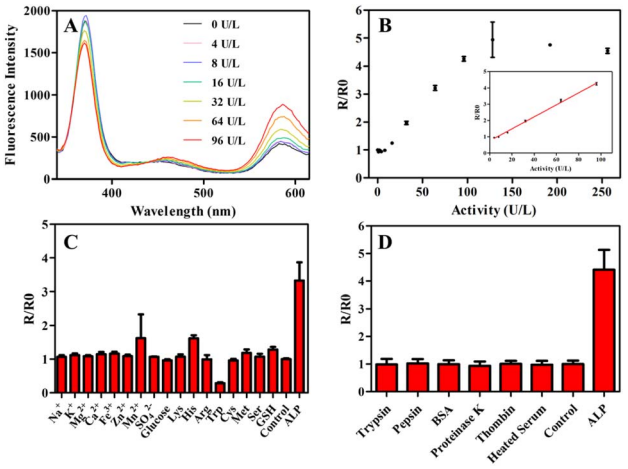

Fig. 3 The linearity and selectivity of ratiometric fluorescent assay of ALP activity based on inner filter effect. (A) The Fluorescence spectra of the incubation system in the presence of ALP (0, 4, 8, 16, 32, 64, 96 U per L). (B) Plots of R/R_0 *versus* ALP activity from 0 to 256 U per L (The inset is the linear relationship from 4 to 96 U per L). R and R_0 are the values of F_{585}/F_{405} in the presence and absence of ALP, respectively. (C) The selectivity for small-molecules. The concentrations of Na^+, K^+ and SO_4^{2-} are 100 mM, Mg^{2+} and Ca^{2+} are 1 mM, Fe^{3+}, Zn^{2+} and Mn^{2+} are 5 μM. The concentrations of amino acids and GSH are 1 mM, and glucose is 10 mM. (D) The selectivity for proteins. Trypsin, pepsin, BSA and proteinase K are 1 mg ml^{-1}, the activity of Thrombin is 100 000 U per L. The inactivate human serum was obtained by heating human serum at 65 °C for 10 min. The activity of ALP is 100 U per L.

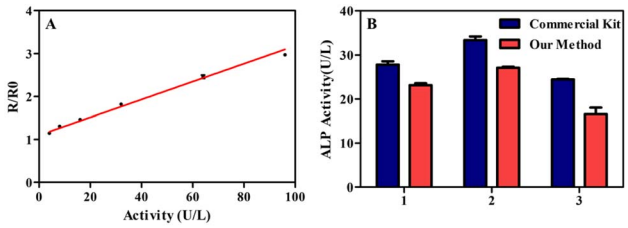

Fig. 4 The performance of ratiometric fluorescent assay in human serum and HepG2 lysate. (A) The linear relationship between R/R_0 and ALP activity in spiked inactivated human serum. R and R_0 are the values of F_{585}/F_{405} in the presence and absence of ALP, respectively. (B) Detection results of serum samples from three adult volunteers by commercial kits and ratiometric fluorescent assay.

Table 1 Recovery rate of ALP in spiked human serum samples (means ± SD, $n = 6$)

Spiked ALP (U/L)	Detected ALP (U per L)	Recovery (%)	RSD (%)
0	9.71 ± 0.16	—	1.7
5	15.20 ± 0.22	109.8	1.4
10	20.86 ± 0.32	111.5	1.5
15	27.22 ± 0.78	116.7	2.9

was selected as the optimum incubation time. In addition, Fig. S4† clearly indicates that the influence of the ratio of Mn:ZnS QDs to ZnSe@ZnS QDs on the detection signals is negligible in the examined range.

Under the optimum conditions, the performance of ratiometric fluorescent assay was investigated. As shown in Fig. 3A, the fluorescence intensity at 585 nm gradually increased and fluorescence intensity at 405 nm decreased with the increasing of ALP activity. A good linear relationship was obtained between ratiometric fluorescence signals (R/R_0) and ALP activity in the range from 4 to 96 U per L (Fig. 3B, $R/R_0 = 0.03688\ C_{ALP} + 0.7513$, $R^2 = 0.9969$) with the detection limit of 0.57 U per L ($3\sigma/k$). The limit of detection (LOD) of proposed rationmetric fluorescent assay was comparable or even lower than previous reported methods (Table S3†). According to the report, the normal level of ALP activity in human serum is about in the range from 20 to 140 U per L,[32] and the sensitivity of ratiometric fluorescent assay completely satisfies the assay of ALP in human serum.

Selectivity of the ratiometric fluorescent assay

In order to validate the selectivity of the detection of ALP, inorganic ions, amino acids, glucose, GSH and proteins were detected in the same conditions as ALP. As shown in Fig. 3C, most of small-molecules investigated did not lead to an obvious rise in R/R_0. Meanwhile, all of the proteins investigated showed negligible effect on R/R_0 (Fig. 3D). Moreover, the influence of inactivated human serum on ratiometric fluorescent signals was also studied, it was impressive that the signals of inactivated human serum extremely approached to the control group. The outstanding selectivity of the detection method indicated great potential for ALP activity detection in human serum.

ALP activity detection in human serum

As shown in Fig. 4A, there was a good linear relationship between R/R_0 and ALP activity (4 to 96 U per L, $R^2 = 0.9907$) in spiked inactivated human serum. To investigate the applicability of the detection method in clinical detection of ALP, the human serum samples from three adult volunteers were detected by commercial kits and ratiometric fluorescent assay. Fig. 4B showed that the results of these two methods were generally similar.

In order to further validate the performance of the ratiometric fluorescent assay for accurately detecting ALP activity in human serum, the spiked human serum samples were detected. The average recovery rate of spiked serum samples was 109.8% to 116.7% (Table 1). These above results confirmed the application prospect of ratiometric fluorescent assay in clinical detection.

ALP activity detection in HepG2 lysate

As far as we know, the up regulation of ALP activity usually appears in certain kinds of tumor cells including HepG2 cells.[33] Therefore, HepG2 cells were used to evaluate the performance of ratiometric fluorescent assay for ALP activity detection in lysate of tumor cells. Fig. 5A illustrates a good linear relationship between ratiometric fluorescence signals (R/R_0) and cell density in the range from 0.2×10^5 to 3.2×10^5 cells per ml. In

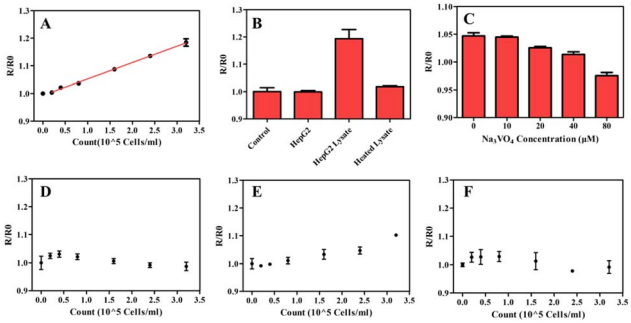

Fig. 5 (A) The linear relationship between R/R_0 and cell density. (B) The effects of different treatments to HepG2 cells (3.2×10^5 cells per ml) on the values of R/R_0. (C) The inhibition of ALP activity in HepG2 lysate (1.0×10^5 cells per ml) caused by different concentrations of Na_3VO_4, and the HepG2 lysate was treated with Na_3VO_4 for 30 min at 4 °C before detection. The relationship between ratiometric fluorescence signals and the cell density of HUVEC (D), L02 (E) and RPMI8226 (F). R and R_0 are the values of F_{585}/F_{405} in the presence and absence of ALP, respectively.

consideration of the low consumption of samples (20 μl), the ALP activity could be detected even the number of HepG2 cells was as low as 400. The HepG2 suspensions without lysis and inactivated lysate of HepG2 cells were also detected under the same conditions, the result shows the signals hardly changed compared with control groups (Fig. 5B). Moreover, the signals of the HepG2 lysate treated with Na_3VO_4 (A classical alkaline phosphatase inhibitor) also obviously decreased with the increasing of concentration of Na_3VO_4 (Fig. 5C). The above results confirmed that there the ratiometric fluorescent assay could distinguish ALP from interfering substances in HepG2 lysate.

In addition, the proposed method was also applied to the detection of ALP activity in different kinds of cell lysates. Fig. 5D–F show the relationship between ratiometric fluorescence signals R/R_0 and the cell density of HUVEC, L02 and RPMI8226, respectively. The results clearly show that the ratiometric fluorescence signal only increased in L02 lysates, which is because ALP produced by normal liver cells is an important source of ALP in human serum. HUVEC lysates could hardly increase the ratiometric fluorescence signal, indicating the low expression of ALP in HUVEC, which is consistent with previous report.[34] Although RPMI8226 is tumor cell line, the results show that RPMI8226 lysate did not lead to elevated detection signals. Actually, previous reports have not shown that myeloma cells have a high expression of ALP,[35] and ALP levels are usually maintained at normal levels or slightly decreased in myeloma patients.[36] In conclusion, the proposed method can distinguish between low and high ALP expression cell lines, and is expected to be applied in the diagnosis of cancer.

Experimental

Chemicals and materials

Zinc stearate (Zn 10–12%), sulfur powder (99.99%), Oleylamine (C18 80–90%), selenium powder (99.9%), glutathione (98%), tritonX-100 (Biochemical reagent), *p*-nitrophenyl phosphate disodium hexahydrate (98%) was purchased from Aladdin (ShangHai, China). Stearic acid (98%), rhodamine 6G(Analytical reagent), sodium orthovanadate (Analytical reagent) were purchased from Macklin (ShangHai, China). Alkaline Phosphatase (from bovine intestinal mucosa), Proteinase K (from tritirachium album limber) were purchased from Sigma (Saint Louis, America). Trypsin (biological reagent), pepsin (Biological reagent), RPMI1640 media were purchased from KeyGen Biotech (NanJing, China). Thrombin (from bovine plasma) and alkaline phosphatase assay kits were purchased from Byetime (ShangHai, China). Human serum was purchased from XinFan Biotech (ShangHai, China). Fetal bovine serum (FBS) was purchased from BIOIND (Israel). Methyl thiazolyl tetrazolium (MTT) was purchased from Biosharp (Hefei, China).

Preparation of Mn:ZnS QDs

Mn:ZnS QDs was prepared based on the reported method with modification.[37] Typically, zinc stearate ($ZnSt_2$, 10 mmol), stearic acid (SA, 10 mmol) and 1-octadecene (ODE, 10 ml) were mixed and heated to 140 °C, and then the Zn stock solution was obtained. $ZnSt_2$ (1 mmol), $MnSt_2$ (0.05 mmol), sulphur powder (5 mmol), oleylamine (OAm, 7.5 mmol) and ODE (50 ml) were added into a 100 ml four-necked flask (Fig. 6A). Then, the reaction mixture was degassed for 20 min by purging nitrogen and kept heating. Once the temperature reached 270 °C, Zn stock solution was added into the reaction mixture at once. Then, the reaction mixture was kept at 250 °C for 30 min and cooled down to room temperature. The crude product was washed for three time with *n*-hexane to remove ODE. To remove extra $ZnSt_2$ and SA, the precipitate was extracted with *n*-hexane, and Mn:ZnS QDs was dissolved in *n*-hexane. The QDs solution was dried at 65 °C to obtain brown oil-dispersible Mn:ZnS QDs (Fig. 6C).

The phase transition of Mn:ZnS QDs was based on previously reported method with modification.[38] The oil-dispersible

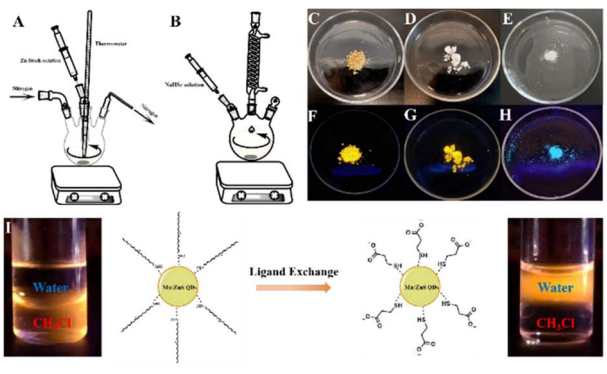

Fig. 6 The devices which were used in the preparation of Mn:ZnS QDs (A) and ZnSe@ZnS QDs (B). The photographs of oil-dispersible Mn:ZnS QDs (C), water-dispersible Mn:ZnS QDs (D) and ZnSe@ZnS QDs (E), respectively. The photographs of oil-dispersible Mn:ZnS QDs (F), water-dispersible Mn:ZnS QDs (G) and ZnSe@ZnS QDs (H) under 254 nm illumination, respectively. The schematic diagram of phase transition between oil-dispersible Mn:ZnS QDs and water-dispersible Mn:ZnS QDs by ligand exchange (I).

Mn:ZnS QDs (1.5 g) was dissolved in chloroform (10 ml), and then 3-mercaptopropionic acid (MPA, 1.6 ml) was added under vigorously stirring. The reaction mixture was sonicated for 30 min and centrifuged for 2 min at 2500 g, then precipitate was washed for three times with chloroform to remove MPA. The precipitate was dispersed in 10 ml solution of tetramethylammonium hydroxide (TMAH, 1 M) and the mixture was centrifuged for 2 min at 2500 g. The supernatant liquid was collected and dried by vacuum overnight at 50 °C. Finally, the white solid was obtained, which was water-dispersible Mn:ZnS QDs (Fig. 6D). Oil- and water-dispersible Mn:ZnS QDs powder have yellow fluorescence under 254 nm wavelength illumination (Fig. 6F and G). The phase transition also confirmed by the migration of fluorescence from chloroform layer to aqueous layer (Fig. 6I). Rhodamine 6G ($\Phi = 95\%$) was selected as reference material for Mn:ZnS QDs. The quantum yields were calculated from the following equation:

$$\Phi s = (OD_s/OD_r) \times (I_s/I_r) \times (\eta_s{}^2/\eta_r{}^2) \times \Phi_r \quad (1)$$

in which the OD, I, η were the absorbance at excitation wavelength, integrated fluorescence intensity and refractive index of solvent, respectively. The excitation wavelengths were set at 275 nm, the ranges of integration were from 450 nm to 700 nm for Mn:ZnS QDs.

Preparation of ZnSe@ZnS QDs

Firstly, Se powder (0.1 mmol), $NaBH_4$ (0.6 mmol) and ultrapure water (1 ml) were added into a 25 ml three-necked flask under nitrogen atmosphere. The mixture was stirred for 40 min at room temperature, and then stood for 10 min in ice bath. After that, NaHSe solution was obtained. In another 250 ml three-necked flask, $ZnSO_4 \cdot 7H_2O$ (0.4 mmol) and glutathione (GSH, 0.5 mmol) were mixed with ultrapure water (100 ml) and the pH was adjusted to 10.5 with NaOH solution (1 M). NaHSe solution was injected into the solution and stirred for 30 min. Finally, the ZnSe QDs was obtained after refluxing for 1.5 h (Fig. 6B).

In a 50 ml three-necked flask, 20 ml of ZnSe QDs solution, $ZnSO_4 \cdot 7H_2O$ (0.1 mmol), MPA (26 μl) were mixed under vigorously stirring and the pH of mixture was adjusted to 10.5 with NaOH solution (1 M). The reaction mixture was stirred vigorously for 1 h and refluxed for another 1 h. The crude product was concentrated by rotary evaporation and nanocrystal was precipitated by adding absolute ethyl alcohol. ZnSe@ZnS QDs was collected after centrifuging for 30 min at 2500 g, then white solid (Fig. 6E) was obtained after drying by vacuum overnight at 50 °C. ZnSe@ZnS QDs powder have blue fluorescence under 254 nm wavelength illumination (Fig. 6H). L-Tryptophan ($\Phi =$ 14%) was selected as reference material for ZnSe@ZnS QDs. The quantum yields were calculated from the eqn (1). The excitation wavelengths were set at 310 nm, the ranges of integration were from 310 nm to 450 nm.

Ratiometric fluorescent assay of ALP activity

The detection of ALP activity based on IFE was performed as the following procedures. Firstly, 20 μl of ALP with different activities was added into 130 μl of incubation buffer (pH 10.0), which contained 50 mM DEA, 1 mM $MgCl_2$ and 600 μM PNPP. The reaction system was incubated at 37 °C for 75 min and allowed to stand at room temperature for 10 min. Then, 50 μl QDs solution containing ZnSe@ZnS QDs (0.1 mg ml^{-1}) and Mn:ZnS QDs (10 mg ml^{-1}) was added. The fluorescence intensity and fluorescence spectra were recorded at the excitation wavelength of 310 nm.

Detection of ALP activity in human serum

All experiments related to human serum were approved by ethics committee of Sir Run Run Hospital of Nanjing Medical University (approval no. 2022-SR-S033). Human serum samples were collected from three adult volunteers, and the informed consent was obtained from all human subjects. The whole blood was standing for 1 h and centrifuged for 10 min at 1500 g and the yellowish serum was obtained. Collected human serum was stored at −20 °C until detection. The procedures of ALP assay in serum samples were the same as above.

Analysis with cell lysate

HepG2, L02, HUVEC and RPMI8226 cells were grown in RPMI1640 supplemented with 10% fetal bovine serum (FBS) and 1% streptomycin/penicillin. The incubator was set at 37 °C with 5% CO_2. The cells were centrifuged for 5 min at 1000 rpm and washed with HEPES buffer (10 mM, pH 7.4) containing 137 mM NaCl and 3 mM KCl. Then 20 μl of lysis buffer (10 mM HEPES, 137 mM NaCl, 3 mM KCl, 0.2% TritonX-100) was added into 100 μl of cell suspension and the mixture was incubated at 4 °C for 30 min. Finally, the lysate was obtained and stored at −80 °C. The detection procedures of lysate remained the same as ALP solution.

Conclusions

We have developed a ratiometric fluorescent assay for ALP activity based on IFE, in which Mn:ZnS QDs and ZnSe@ZnS QDs responded to the changes of concentrations of PNPP and PNP and led an enhancement of ratiometric fluorescence signals (F_{585}/F_{405}) with the increasing of ALP activity. The method showed high sensitivity with a detection limit of 0.57 U per L and consumed less samples impressively, the method showed excellent specificity in biological matrix, which contributed to a simple detection process without any pre-treatment of samples. In the detection of real human serum samples, the performance of ratiometric fluorescent assay was close to commercial kits. Moreover, the proposed method was successfully applied to the determination of ALP activity in HepG2 cells. Therefore, the ratiometric fluorescent assay based on IFE not only provided a sensitive, specific and simple approach to clinical ALP activity detection, but it also provided a novel strategy for diagnosis of diseases.

Conflicts of interest

The authors declare that they have no known competing financial interests or personal relationships that could have appeared to influence the work reported in this paper.

Acknowledgements

This study was supported by the Open Project Program of Double first-class construction project (No. CPU2022QZ16).

Notes and references

1 J. L. Millán and M. P. Whyte, *Calcif. Tissue Int.*, 2016, **98**, 398–416.
2 P. Dua, H. S. Kang, S. M. Hong, M. S. Tsao, S. Kim and D. K. Lee, *Cancer Res.*, 2013, **73**, 1934–1945.
3 Y. Hu, Y. Miao, J. Zhang, Y. Chen, L. Qiu, J. Lin and D. Ye, *Nano Lett.*, 2021, **21**, 10377–10385.
4 H. Li, Q. Yao, F. Xu, Y. Li, D. Kim, J. Chung, G. Baek, X. Wu, P. F. Hillman, E. Y. Lee, H. Ge, J. Fan, J. Wang, S. J. Nam, X. Peng and J. Yoon, *Angew. Chem., Int. Ed.*, 2020, **59**, 10186–10195.
5 N. Hildebrandt, C. M. Spillmann, W. Russ Algar, T. Pons, M. H. Stewart, E. Oh, K. Susumu, S. A. Díaz, J. B. Delehanty and I. L. Medintz, *Chem. Rev.*, 2017, **117**, 536–711.
6 P. Wu and X. P. Yan, *Chem. Soc. Rev.*, 2013, **42**, 5489–5521.
7 J. Chen, F. Xu, H. Jiang, Y. Hou, Q. Rao, P. Guo and S. Ding, *Food Chem.*, 2009, **113**, 1197–1201.
8 M. B. Gholivand, E. Ahmadi and M. Mavaei, *Sens. Actuators, B*, 2019, **299**, 126975.
9 Y. T. Yang, J. L. Liu, M. F. Sun, R. Yuan and Y. Q. Chai, *Anal. Chem.*, 2022, **94**, 6874–6881.
10 J. J. Wang, C. Zheng, Y. Z. Jiang, Z. Zheng, M. Lin, Y. Lin, Z. L. Zhang, H. Wang and D. W. Pang, *Anal. Chem.*, 2020, **92**, 830–837.
11 Y. Miao, X. Sun, J. Lv and G. Yan, *ACS Appl. Mater. Interfaces*, 2019, **11**, 2264–2272.
12 Y. H. Lao, C. W. Chi, S. M. Friedrich, K. Peck, T. H. Wang, K. W. Leong and L. C. Chen, *ACS Appl. Mater. Interfaces*, 2016, **8**, 12048–12055.
13 S. Chen and P. I. Imoukhuede, *Anal. Chem.*, 2019, **91**, 7603–7612.
14 G. Mao, Y. Ma, G. Wu, M. Du, S. Tian, S. Huang, X. Ji and Z. He, *Anal. Chem.*, 2021, **93**, 777–783.
15 P. Wu, X. Hou, J. J. Xu and H. Y. Chen, *Nanoscale*, 2016, **8**, 8427–8442.
16 S. Chen, Y. L. Yu and J. H. Wang, *Anal. Chim. Acta*, 2018, **999**, 13–26.
17 J. Ge, Z. Qi, L. Zhang, X. Shen, Y. Shen, W. Wang and Z. Li, *Nanoscale*, 2020, **12**, 808–814.
18 J. Zhang, R. Zhou, D. Tang, X. Hou and P. Wu, *TrAC, Trends Anal. Chem.*, 2019, **110**, 183–190.
19 E. Sheng, Y. Lu, Y. Tan, Y. Xiao, Z. Li and Z. Dai, *Anal. Chem.*, 2020, **92**, 4364–4370.
20 S. Zhu, X. Yan, J. Sun, X. E. Zhao and X. Wang, *Talanta*, 2019, **200**, 163–168.
21 L. Zhang, J. Q. Chen, M. F. Hong, R. P. Liang and J. D. Qiu, *Analyst*, 2020, **145**, 2570–2579.
22 M. Cai, C. Ding, F. Wang, M. Ye, C. Zhang and Y. Xian, *Biosens. Bioelectron.*, 2019, **137**, 148–153.
23 D. Li, J. Qin, Q. Xu and G. Yan, *Sens. Actuators, B*, 2018, **274**, 78–84.
24 G. Li, H. Fu, X. Chen, P. Gong, G. Chen, L. Xia, H. Wang, J. You and Y. Wu, *Anal. Chem.*, 2016, **88**, 2720–2726.
25 A. Bigdeli, F. Ghasemi, S. Abbasi-Moayed, M. Shahrajabian, N. Fahimi-Kashani, S. Jafarinejad, M. A. Farahmand Nejad and M. R. Hormozi-Nezhad, *Anal. Chim. Acta*, 2019, **1079**, 30–58.
26 J. Qian, Z. Teng, J. Wang, L. Zhang, T. Cao, L. Zheng, Y. Cao, W. Qin, Y. Liu and H. Guo, *ACS Sens.*, 2020, **5**, 2806–2813.
27 X. Yue, J. Wang, J. Han, B. Wang and X. Song, *Chem. Commun.*, 2020, **56**, 2849–2852.
28 J. F. Suyver, S. F. Wuister, J. J. Kelly and A. Meijerink, *Nano Lett.*, 2001, **1**, 429–433.
29 R. Toufanian, X. Zhong, J. C. Kays, A. M. Saeboe and A. M. Dennis, *Chem. Mater.*, 2021, **33**, 7527–7536.
30 V. G. Reshma, A. Sabareeswaran, K. S. Rajeev and P. V. Mohanan, *Food Chem. Toxicol.*, 2020, **145**, 111718.
31 H. Zimmermann, M. Zebisch and N. Sträter, *Purinergic Signalling*, 2012, **8**, 437–502.
32 Y. Zhang, H. Li, D. Xie, J. Li, Y. Zhang, B. Wang, C. Liu, Y. Song, X. Wang, Y. Huo, F. F. Hou, X. Xu and X. Qin, *Front. Cardiovasc. Med.*, 2021, **8**, 749196.
33 A. Nowrouzi and R. Yazdanparast, *Biochem. Biophys. Res. Commun.*, 2005, **330**, 400–409.
34 Y. Bo, L. Yan, Z. Gang, L. Tao and T. Yinghui, *Cell Biol. Int.*, 2012, **36**, 909–915.
35 B. Zdzisińska, A. Bojarska-Junak, A. Walter-Croneck and M. Kandefer-Szerszeń, *Arch. Immunol. Ther. Exp.*, 2010, **58**, 153–163.
36 O. Annibali, M. T. Petrucci, D. Santini, V. Bongarzoni, M. Russano, F. Pisani, O. Venditti, F. Pantano, A. Rago, A. Siniscalchi, E. Cerchiara, L. Franceschini, L. de Rosa, M. Mariani, S. Andriani, L. Cudillo, M. Garcia, M. Cantonetti, S. Mohamed, B. Anaclerico, T. Caravita, F. Stocchi, G. Cimino, S. Gumenyuk, F. Vozella and G. Avvisati, *J. Bone Oncol.*, 2021, **26**, 100338.
37 B. B. Srivastava, S. Jana, N. S. Karan, S. Paria, N. R. Jana, D. D. Sarma and N. Pradhan, *J. Phys. Chem. Lett.*, 2010, **1**, 1454–1458.
38 N. Pradhan, D. M. Battaglia, Y. Liu and X. Peng, *Nano Lett.*, 2007, **7**, 312–317.